Available online at www.sciencedirect.com
ScienceDirect
Metabolic Engineering 9 (2007) 177–192
METABOLIC ENGINEERING
www.elsevier.com/locate/ymben

Determining *Actinobacillus succinogenes* metabolic pathways and fluxes by NMR and GC-MS analyses of ^{13}C-labeled metabolic product isotopomers

James B. McKinlay[a], Yair Shachar-Hill[b], J. Gregory Zeikus[a,c], Claire Vieille[c,*]

[a]*Department of Microbiology and Molecular Genetics, Michigan State University, East Lansing, MI 48824, USA*
[b]*Department of Plant Biology, Michigan State University, East Lansing, MI 48824, USA*
[c]*Department of Biochemistry and Molecular Biology, Michigan State University, East Lansing, MI 48824, USA*

Received 31 July 2006; received in revised form 12 October 2006; accepted 31 October 2006
Available online 17 November 2006

Abstract

Actinobacillus succinogenes is a promising candidate for industrial succinate production. However, in addition to producing succinate, it also produces formate and acetate. To understand carbon flux distribution to succinate and alternative products we fed *A. succinogenes* [1-^{13}C]glucose and analyzed the resulting isotopomers of excreted organic acids, proteinaceous amino acids, and glycogen monomers by gas chromatography-mass spectrometry and nuclear magnetic resonance spectroscopy. The isotopomer data, together with the glucose consumption and product formation rates and the *A. succinogenes* biomass composition, were supplied to a metabolic flux model. Oxidative pentose phosphate pathway flux supplied, at most, 20% of the estimated NADPH requirement for cell growth. The model indicated that NADPH was instead produced primarily by the conversion of NADH to NADPH by transhydrogenase and/or by NADP-dependent malic enzyme. Transhydrogenase activity was detected in *A. succinogenes* cell extracts, as were formate and pyruvate dehydrogenases, which the model suggested were contributing to NADH production. Malic enzyme activity was also detected in cell extracts, consistent with the flux analysis results. Labeling patterns in amino acids and organic acids showed that oxaloacetate and malate were being decarboxylated to pyruvate. These are the first in vivo experiments to show that the partitioning of flux between succinate and alternative fermentation products can occur at multiple nodes in *A. succinogenes*. The implications for designing effective metabolic engineering strategies to increase *A. succinogenes* succinate production are discussed.

Keywords: *Actinobacillus succinogenes*; Succinate; Metabolic flux analysis; Biomass composition; Oxaloacetate decarboxylase; Malic enzyme; Transhydrogenase

1. Introduction

Declining oil reserves, rising petrochemical prices, and the environmental impact of oil-based industries have prompted the development of bio-based processes for fuel and chemical production (Wilke, 1995, 1999). Industrial-scale microbial processes are meeting the global demands for a variety of amino acids, organic acids, vitamins, and antibiotics (Wilke, 1999). Succinate is produced petrochemically from butane to satisfy a specialty chemical market, but it can also be produced from microbial fermentations (Zeikus et al., 1999). More importantly, bio-based succinate could replace a large petrochemical-based commodity chemical market for making bulk chemicals including 1,4-butanediol (a precursor to "stronger-than-steel" and biodegradable plastics), ethylene diamine disuccinate (a biodegradable chelator), diethyl succinate (a "green" solvent replacement for methylene chloride), and adipic acid (a nylon precursor) (Zeikus et al., 1999). In addition to being based on renewable resources, bio-based succinate production has the environmental

*Corresponding author. Fax: +1 517 353 9334.
E-mail address: vieille@msu.edu (C. Vieille).

1096-7176/$ - see front matter © 2006 Elsevier Inc. All rights reserved.
doi:10.1016/j.ymben.2006.10.006

benefit of using CO_2, a greenhouse gas, as a substrate. Developing a more cost-effective industrial succinate fermentation to replace the butane-based commodity maleic anhydride will require advances on several fronts. In particular, it will require developing organisms that produce high succinate concentrations at high rates.

The capnophilic bacterium, *Actinobacillus succinogenes*, is a promising biocatalyst for industrial succinate production. While *A. succinogenes* produces some of the highest succinate concentrations ever reported (Guettler et al., 1996a, b), it does so as part of a mixed acid fermentation, producing high concentrations of formate and acetate as well. Therefore, it is desirable to genetically engineer *A. succinogenes* to produce succinate as the sole fermentation end product.

Metabolic engineering is most effective when it is based on an understanding of the pathways involved and of how the fluxes through those pathways are controlled (Fell, 1997; Stephanopoulos et al., 1998). Knowledge of *A. succinogenes* metabolism comes from fermentation balances, from in vitro enzyme assays (McKinlay et al., 2005; van der Werf et al., 1997), and, more recently, from its genome sequence (McKinlay et al., manuscript in preparation., http://genome.ornl.gov/microbial/asuc/). A simplified map of *A. succinogenes* central metabolism is depicted in Fig. 1. Previous data suggest that *A. succinogenes* ferments glucose to phosphoenolpyruvate (PEP) by glycolysis and the oxidative pentose phosphate pathway (OPPP) (van der Werf et al., 1997). PEP is thought to serve as the branchpoint between the formate-, acetate-, and ethanol-producing pathway (C_3 pathway), and the succinate-producing (C_4) pathway. Malic enzyme and oxaloacetate (OAA) decarboxylase activities measured in vitro (van der Werf et al., 1997) suggest that malate and OAA can also serve as branch points between the C_3 and C_4 pathways. The presence of these activities and others in vivo, such as those of the Entner–Doudoroff (ED) and glyoxylate pathways (for which questionable in vitro activities were detected [van der Werf et al., 1997]), must be determined to develop effective *A. succinogenes* engineering strategies.

^{13}C-labeling studies are a useful approach for understanding the in vivo workings of metabolism (Ratcliffe and Shachar-Hill, 2006; Wiechert, 2001). Knowledge resulting from these techniques has been used to guide the metabolic engineering of industrial microbes, such as vitamin-producing *Bacillus subtilis* (Dauner et al., 2002; Sauer et al., 1997; Zamboni et al., 2003) and amino acid-producing *Corynebacterium glutamicum* (Koffas et al., 2003; Park et al., 1997; Petersen et al., 2000). ^{13}C-labeling studies can distinguish fluxes through different pathways when these fluxes result in different positional isotopic enrichments in metabolic intermediates. These labeling patterns are imprinted on metabolic products (e.g., proteinaceous amino acids and excreted organic acids) and can be analyzed by gas chromatography-mass spectrometry (GC-MS) and nuclear magnetic resonance spectroscopy (NMR). We recently developed a chemically defined growth medium that makes ^{13}C-labeling experiments with *A. succinogenes* possible (McKinlay et al., 2005). Here we describe the use of [1-^{13}C]glucose to obtain an *A. succinogenes* metabolic flux map based on analyses of its cell composition, extracellular fluxes, and isotopomers of amino acids, organic acids, and glycogen monomers.

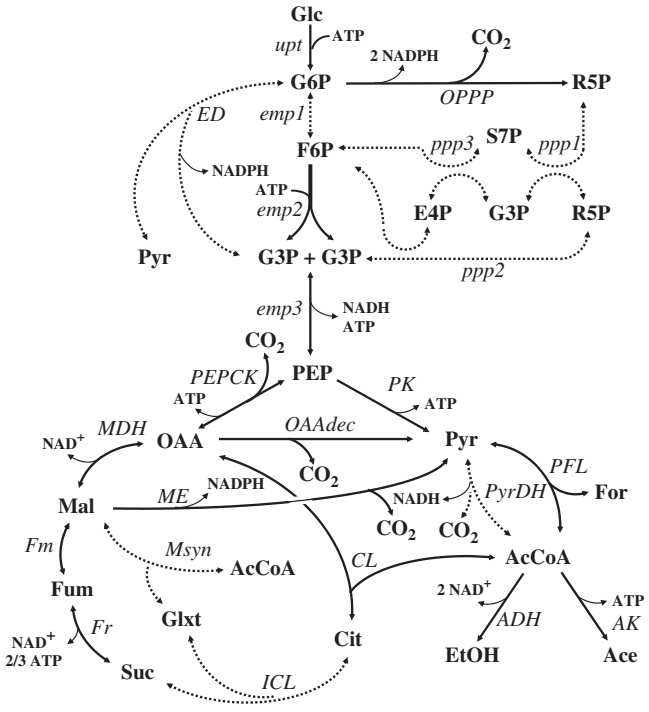

Fig. 1. *A. succinogenes* metabolic pathways addressed in this study. Solid lines: pathways or reactions for which enzyme activity was detected in vitro; dotted lines: pathways or reactions where no activity or uncertain activity was detected in vitro (van der Werf et al., 1997). Unidirectional arrows: fluxes considered to be unidirectional (all other fluxes are considered to be reversible). The C_4 pathway is defined as: PEP→OAA→Mal→Fum→Suc. The C_3 pathway is defined as: PEP→Pyr→AcCoA→Ace + EtOH. Alternative PPP reactions, cysteine and methionine degradation pathways, and amino acid synthesis pathways are not shown (Supplementary material). It was assumed that 0.67 ATP is produced per fumarate reductase reaction based on data from *Wolinella succinogenes* (Kroger et al., 2002). Metabolites: AcCoA, acetyl-coenzymeA; Ace, acetate; Cit, citrate; EtOH, ethanol; E4P, erythrose-4-phosphate; For, formate; Fum, fumarate; F6P, fructose-6-phosphate; Glc, glucose; Glxt, glyoxylate; G3P, glyceraldehyde-3-phosphate; G6P, glucose-6-phosphate; Mal, malate; OAA, oxaloacetate; PEP, phosphoenolpyruvate; Pyr, pyruvate; R5P, pentose-phosphates, Suc, succinate; S7P, sedoheptulose-7-phosphate. Pathways and reactions: *ADH*, alcohol dehydrogenase; *AK*, acetate kinase; *CL*, citrate lyase; *ED*, Entner–Doudoroff pathway; *emp1*, 2, and 3, Embden–Meyerhoff–Parnas (EMP) or glycolytic reactions; *Fm*, fumarase; *FR*, fumarate reductase; *ICL*, isocitrate lyase and aconitase; *MDH*, malate dehydrogenase; *ME*, malic enzyme; *Msyn*, malate synthase; *OAAdec*, oxaloacetate decarboxylase; *OPPP*, oxidative pentose phosphate pathway; *PEPCK*, PEP carboxykinase; *PFL*, pyruvate formate-lyase; *PK*, pyruvate kinase and PEP:glucose phosphotransferase system (PTS); *ppp1* and 2, transketolase; *ppp3*, transaldolase; *PyrDH*, pyruvate dehydrogenase or PFL coupled with formate dehydrogenase; *upt*, glucose phosphorylation by hexokinase and PTS.

2. Materials and methods

2.1. Chemicals, bacteria, and culture conditions

All chemicals were purchased from Sigma-Aldrich (St. Louis, MO) unless stated otherwise. *A. succinogenes* type strain 130Z (ATCC 55618) was purchased from the American Type Culture Collection (Manassas, VA) and adapted to growth in AM3 as described (McKinlay et al., 2005). AM3 is a chemically defined medium containing Cys, Met, and Glu, which are required for *A. succinogenes* growth. Cultures were grown in 11-ml volumes of AM3 in 28-ml anaerobic test tubes or in 60-ml volumes in 150-ml serum vials. Anoxic AM3 contained 150 mM $NaHCO_3$ and 50 mM glucose, and was prepared as described (McKinlay et al., 2005). Cultures were incubated at 37 °C with shaking at 250 rpm.

2.2. Growth and sampling conditions in the presence of [1-^{13}C]glucose

A starter culture was grown from a glycerol frozen stock in AM3 to an OD_{660} of 1.0. The starter culture was harvested, washed once, and resuspended in an equal volume of the AM3 phosphate buffer. Nine 11-ml volumes of AM3 containing 50 mM [1-^{13}C]glucose (99%, Cambridge Isotope Laboratories, Cambridge, MA), instead of unlabeled glucose, were each inoculated with 0.1 ml of the cell suspension to give a starting OD_{660} of ~0.01. Unlabeled biomass accounted for only 0.5–1.8% of the total biomass at the time of harvesting. Growth was monitored using a Spectronic 20 spectrophotometer (Bausch and Lomb, Rochester, NY) to calculate growth rates. A 1-ml sample was taken 4.5 h into growth to serve as a '0 time point' sample, rather than at the time of inoculation to account for any lag phase. This sample was used for a more accurate OD_{660} measurement using a Beckman DU 650 spectrophotometer (Fullerton, CA). It was also analyzed by high-performance liquid chromatography (HPLC) to determine glucose and product concentrations. Culture growth was stopped by chilling on ice as follows: three tubes were stopped at 0.5 OD_{660}, three at 1.0 OD_{660}, and three at 1.5 OD_{660}. Cell densities were recorded, then cultures were harvested by centrifugation at 4 °C. The supernatants were stored at −70 °C, as was the biomass after two washes with 0.9% NaCl at 4 °C.

2.3. HPLC analysis of glucose and products and GC analysis of headspace gas

HPLC was performed on culture supernatants as described (McKinlay et al., 2005). A negative HCO_3^- peak interfered with ethanol peak integration. To improve the ethanol measurement accuracy, subsamples were mixed 1:1 with 150 mM H_2SO_4 to release HCO_3^- as CO_2 before analysis. Untreated samples were used to quantify glucose, succinate, formate, acetate, and fumarate. GC was used to analyze culture headspace for H_2 using a Shimadzu GC-2014 (Columbia, MD) equipped with an 80/100 Porapak Q column and a thermal conductivity detector.

2.4. Determination of extracellular fluxes

Specific glucose consumption and product formation rates (i.e., extracellular fluxes) were calculated as described (Sauer et al., 1999) using the equation $r_p = Y_{XP}\mu$, where r_p is the specific product formation rate, Y_{XP} is the amount of product produced per gram of biomass, and μ is the growth rate. The same equation was used for glucose consumption. All flux data were obtained during exponential growth, during which the growth rate and extracellular fluxes are constant.

2.5. GC-MS analysis of amino acids and organic acids

Amino acid preparation and GC-MS analysis were based on the methods of Schwender et al. (2003) and Dauner and Sauer (2000). All drying and evaporation steps were performed under a stream of N_2. Each cell pellet from 8.4 ml of culture was resuspended in 1 ml of distilled water and lysed by six freeze-thaw cycles (−70 °C/30 °C). The lysates were centrifuged, then 600 µl aliquots of supernatant were transferred to 1.5-ml screw-cap conical tubes and concentrated to 100 µl under vacuum. Proteins were hydrolyzed by adding 333 µl of 6 N HCl to each sample and incubating at 110 °C for 24 h under Ar. HCl was then evaporated to near-dryness at 55 °C, then samples were diluted with 1 ml of 0.01 N HCl, and applied to a Dowex 50Wx8-100 cation exchange column. Amino acids were eluted with 1 N NH_4OH and dried at 55 °C. Samples were then dissolved in 0.1 ml of 0.01 N HCl. Amino acid concentrations were estimated by spotting 10- and 100-fold dilutions of the samples and an amino acid standard onto silica gel plates and comparing the color intensities after staining with a ninhydrin spray solution and incubating at 80 °C for 10 min. Volumes containing 100–200 µg of amino acids were transferred to glass vials and dried at 25 °C. To derivatize the amino acids for GC-MS analysis, 800 µl of methylene chloride was added to each sample and evaporated to remove trace amounts of water. Acetonitrile and *N*-(*tert*-butyldimethylsilyl)-*N*-methyl-trifluoroacetamide (MTBSTFA) (200 µl each) were then added to the samples under Ar. Vials were capped and incubated at 25 °C for 30 min, then at 120 °C for 1 h. Samples were evaporated to near dryness at 25 °C before being diluted with 400 µl of 20:1 acetonitrile:MTBSTFA, and run on GC-MS. Succinate and fumarate in supernatants were derivatized by the same method but without column purification, and their concentrations were determined by HPLC.

GC-MS was performed using an Agilent 5973 inert MSD benchtop quadrapole mass spectrometer (Palo Alto, CA) at the MSU Mass Spectrometry facility. Derivatized compounds in 1-µl injections were separated on a 60-m

DB5MS column. The inlet temperature was 280 °C. The oven temperature started at 100 °C for 4 min, was then raised by 5 °C/min to 200 °C, then by 10 °C/min to 300 °C, and held at 300 °C for 10 min. *Tert*-butyldimethylsilyl (TBDMS)-amino acid and organic acids were identified using described fragmentation patterns (Dauner and Sauer, 2000) and unlabeled standards.

2.6. NMR analysis of organic acids, alanine, and glucose monomers from glycogen

Prior to NMR analysis, organic acids were separated from glucose and ethanol on a Dowex 1×8-200 anion exchange column. Organic acids were eluted with 1 M $HClO_4$. The eluate was made alkaline by adding K_2CO_3 until CO_2 bubbles stopped forming. The $KClO_4$ precipitate was pelleted by centrifugation and the supernatant was lyophilized and dissolved in D_2O. Amino acids were obtained from hydrolyzed proteins as described above but, prior to hydrolysis, the proteins were precipitated with trichloroacetic acid (25% final concentration) on ice for 30 min, pelleted by centrifugation, washed twice with ice-cold acetone, air-dried, and resuspended in 100 µl water. After hydrolysis, amino acids were partially purified, dried, and dissolved in D_2O. Glucose monomers were prepared from glycogen by resuspending the pellets from centrifuged cell lysates in 50 mM sodium acetate (pH 4.5), boiling for 5 min, then digesting with *Pseudomonas amyloderamosa* isoamylase (E.C. 3.2.1.68) and *Aspergillus niger* amyloglucosidase (E.C. 3.2.1.3) for 24 h at 40 °C with occasional mixing. Cell debris was pelleted by centrifugation, and the supernatant was applied to a Dowex 1×8-200 anion exchange column. The flow-through was lyophilized and redissolved in D_2O.

All compounds were analyzed by ^{1}H-NMR and ^{1}H-decoupled ^{13}C-NMR using a Varian VXR 500 MHz spectrometer with a 5-mm ^{13}C–^{1}H switchable probe at the MSU Max T. Rodgers NMR facility. For ^{13}C-NMR, ^{1}H-decoupling was applied only during acquisition, and recycle times were 60–120 s to allow for full relaxation. After determining that there were no statistical differences in the relative ^{1}H-NMR peak intensities between samples originating from different cell concentrations (see Results), the organic acid samples originating from all OD_{660} 0.5 and OD_{660} 1.0 cultures were combined into a single sample to decrease ^{13}C-NMR run times. Organic acid samples originating from the OD_{660} 1.5 cultures were not pooled for ^{13}C-NMR. All samples were pooled for glucose and Ala measurements. NMR peak assignments were based on spectra found at www.aist.go.jp/RIODB/SDBS/(Japanese National Institute of Advanced Industrial Science and Technology, December 2005) and on spectra of unlabeled standards.

2.7. Metabolic modeling and flux analysis

The initial *A. succinogenes* metabolic model (Fig. 1) is based on *A. succinogenes* enzyme activities (van der Werf et al., 1997), and on sequences in the *A. succinogenes* draft genome sequence. The tricarboxylic acid (TCA) cycle was omitted because it was shown that *A. succinogenes* cannot synthesize α-ketoglutarate when grown in AM3, indicating at least two missing TCA cycle enzyme activities (McKinlay et al., 2005). Glucose uptake was not constrained to the conversion of PEP to pyruvate (i.e., by the PEP:glucose phosphotransferase system [PTS]) to allow for glucokinase activity. Both PTS and glucokinase activities were detected in *A. succinogenes* (van der Werf et al., 1997), and the PTS does not appear to be the main glucose uptake mechanism at high glucose concentrations (Kim and Vieille, submitted). Pyruvate carboxylating activities were omitted, because no pyruvate carboxylase gene was found in any *Pasteurellaceae* genome sequence, and *A. succinogenes* pyruvate formate-lyase mutants excrete pyruvate (Guettler et al., 1996a), suggesting that *A. succinogenes* cannot carboxylate pyruvate. Redox balance constraints were omitted to allow for transhydrogenase activity.

AM3 contains unlabeled Glu, Cys, Met, and vitamins that could potentially enter amino acid or central metabolic pathways and affect our interpretation of the isotopomer data set. Glu cannot affect the isotopomer data set for several reasons. First, it is normally catabolized via α-ketoglutarate, which is disconnected from central metabolism in *A. succinogenes* (McKinlay et al., 2005). Second, there is only enough Glu supplied to meet the biosynthetic requirements for Glu and its derivatives, Gln, Pro, Arg, and polyamines (estimated from Table 1 values). While unlabeled Glu directly affects the isotopomer distribution of Gln, Pro, and Arg (Glx and Pro are ~100% unlabeled, Table 2), these amino acid isotopomers are not used in our flux analysis, and not enough Glu is provided to affect other metabolic pathways. The amount of vitamins supplied is also too low to impact our isotopomer measurements, representing only 0.28% of the carbon consumed as glucose by the lowest cell density culture and 0.07% of that consumed by the highest cell density culture. Cys and Met are supplied at 4- and 5-fold excess, respectively, and together account for 1.3% of the total supplied carbon. For this reason, we included Cys and Met degradation pathways in our model based on those found at Metacyc (i.e., Cys → pyruvate; Met → oxobutanoate → Thr → Asp → OAA; www.metacyc.com).

The model is simplified for flux analysis by grouping metabolites that are assumed to be in rapid equilibrium (e.g., pentose phosphates in the pentose phosphate pathway [PPP]), or that are undistinguishable by labeling (e.g., all metabolites in glycolysis between glyceraldehyde-3-phosphate [G3P] and 3-phosphoglycerate). Anabolic fluxes were based on the *A. succinogenes* biomass composition (Table 1). The standard deviation for all anabolic fluxes was set to 10% of the flux value, which is the average standard deviation determined from replicate samples for all measured biomass components, and which takes into account the standard deviation for the dry cell weight determination. The biosynthetic origin of amino acid

Table 1
A. succinogenes metabolic intermediate and cofactor requirements for biosynthesis

	% of dry cell wt.	μmols per g biomass												
		ATP[a]	NADH	NADPH	NH_3	G6P	F6P	R5P	E4P	G3P	3PG	PEP	Pyr	AcCoA	OAA
Protein	56.8	22,689													
Ala	6.0			671	671								671		
Arg	2.5	1009	−144	432	432										
Asx[b]	5.6	634		423	634										423
Cys[b]	0.9														
Glx[b]	6.0	203			203										
Gly	5.8		−768	768	768						768				
His	1.1	435	−218	73	218			73							
Ile	3.1	480		1201	240								240		240
Leu	4.9		−374	747	374								747	374	
Lys	3.9	528		1056	528								264		264
Met	1.1														
Phe	2.3	139		277	139				139			277			
Pro	2.3	196		392	196										
Ser	2.2		−211	211	211						211				
Thr	2.9	492		737	246										246
Trp[b]	0.6	149	−60	90	60			30	30			30			
Tyr[b]	1.4	75	−75	150	75				75			150			
Val	4.3			727	363								727		
RNA[c]	14.2	4304	−583	317	1536			415			194				221
DNA[d]	4.4	1670	−195	274	498			135			65				70
Glycogen	6.6	366				366									
Lipid[e]	8.8	2081	−99	3688	99					66	99			2098	
LPS	4.7	1073	0	817	33	44	49	33		33	33	33		457	
PG	3.5	192		269	230		77					38	115	77	38
Polyamines[f]	0.4	119		119	59										
Uptake[g]: NH_3		7813													
PO_4^{2-}		1108													
K^+		190													
Amino acids		985													
		ATP	NADH	NADPH	NH_3	G6P	F6P	R5P	E4P	G3P	3PG	PEP	Pyr	AcCoA	OAA
TOTAL	99.5[h]	46,930	−2727	13,439	7813	410	126	686	244	99	1370	528	2764	3006	1502

Table 1 values were corrected for Glu, Cys, and Met, which are supplied in AM3.

[a]ATP needs for polymerization reactions were assumed to be the same as in *E. coli* (Ingraham et al., 1983), but adjusted for percentage of dry cell weight.

[b]Gln and Asn were oxidized to Glu and Asp during hydrolysis and Cys and Trp were destroyed. Cys and Trp values were based on *E. coli* values (Ingraham et al., 1983). A correction factor was applied to Tyr to account for average recoveries of 70%.

[c]The values were derived using an RNA NTP composition based on that of *A. succinogenes* ribosomal RNA.

[d]The values were derived using a DNA dNTP composition based on the GC content of *A. succinogenes* (Guettler et al., 1999).

[e]The phospholipid composition was assumed to be 25% phosphatidylglycerol and 75% phosphatidylethanolamine. The values were derived using the *A. succinogenes* fatty acid composition, which was measured to be (in percent of total lipid mass): 14:0, 11; 3-OH-14:0, 3; 16:0, 35; 16:1, 37; 18:0, 1; 18:1, 3; and 18:2, 10.

[f]The polyamine requirement was assumed to be the same as for *E. coli* (Ingraham et al., 1983).

[g]A stoichiometry of 1 ATP per NH_3, PO_4^{2-}, or amino acid transported was assumed. The ATP requirement for K^+ transport was assumed to be 190 μmol per g biomass^{-1} (Stouthamer, 1979).

[h]Unaccounted for biomass is assumed to be composed of metabolites and inorganic ions.

carbon atoms from their metabolic precursors was based on constraints described by Szyperski (1995).

Extracellular fluxes, and NMR and GC-MS data sets used were averages of measurements on all nine cultures with the exception of a few samples that were pooled for NMR analyses (see NMR methods section). Mass isotopomer standard deviations for individual amino acid fragments from all nine cultures were typically <1%. To more closely reflect biological variability, standard deviations for mass isotopomers were raised to 2.6%. This value was the standard deviation between mass isotopomers that are expected to be identical (i.e., between Ala, Asp, Ser, and Thr M-57 fragment x+0 mass isotopomers). The averaged data were applied to several versions of an *A. succinogenes* metabolic model (Fig. 1) using ^{13}C-*Flux* software (Wiechert et al., 2001). The model variations were: the presence and absence of ED and glyoxylate pathways, and alternative PPP reactions (Kleijn et al., 2005; van Winden et al., 2001), as well as grouping or separating OAA and malate pools. ^{13}C-*Flux* uses a

Table 2
Mass isotopomer distributions of TBDMS-amino acid and -organic acid fragments

Product	Fragment	Carbons	Mass isotopomer distributions[a] (% of product population)					
			X+0	X+1	X+2	X+3	X+4	X+5
Ala	M-57	1–3	54.0±0.4 (52.0)	45.8±0.3 (48.0)	0.1±0.0 (0.0)	0.1±0.1[b]		
	M-85	2–3	53.8±1.3 (52.2)	46.0±1.2 (47.8)	0.4±0.1 (0.0)			
Asx	M-57	1–4	51.4±0.5 (51.8)	47.5±0.4 (48.0)	0.6±0.2 (0.2)	0.4±0.1[b]	0.2±0.0[b]	
	M-85	2–4	52.5±0.5 (52.0)	47.4±0.4 (47.9)	0.1±0.2 (0.1)	0.1±0.1[b]		
	M-159	2–4	52.9±0.6 (52.0)	46.8±0.5 (47.9)	−0.2±0.1 (0.1)	0.5±0.1[b]		
	f302	1–2	93.7±1.2 (93.4)	6.6±0.8 (6.6)	−0.3±0.1 (0.0)			
Glx[b]	M-57	1–5	101.2±1.1	0.1±0.0	−0.2±0.7	−1.3±2.4	0.2±1.0	0.1±0.1
	M-85	2–5	101.0±0.2	−0.2±0.0	−0.4±0.2	0.1±0.3	−0.5±0.5	
	M-159	2–5	99.8±0.2	0.0±0.0	0.3±0.1	0.0±0.0	−0.1±0.1	
Gly	M-57	1–2	98.7±0.3 (98.8)	1.2±0.2 (1.2)	0.0±0.0 (0.0)			
	M-85	2	99.3±0.3 (99.1)	0.7±0.1 (0.9)				
Ile	M-85	2–6	27.8±0.5 (27.1)	49.1±0.4 (49.8)	23.7±0.3 (23.0)	0.1±0.2 (0.1)	−0.8±0.7[b]	0.1±0.3[b]
	M-159	2–6	27.4±0.3 (27.1)	48.9±0.2 (49.8)	23.5±0.2 (23.0)	0.2±0.0 (0.1)	0.1±0.0[b]	−0.0±0.0[b]
Leu	M-85	2–6	17.7±0.8 (15.5)	38.5±0.4 (40.1)	33.7±0.4 (34.5)	10.0±0.1 (9.9)	0.0±0.0[b]	0.1±0.1[b]
	M-159	2–6	16.6±0.4 (15.5)	38.2±0.3 (40.1)	34.1±0.3 (34.5)	10.4±0.1 (9.9)	0.2±0.0[b]	0.5±0.2[b]
Met[b]	M-57	1–5	97.6±0.9	0.4±0.0	−0.4±0.2	0.6±0.3	0.6±0.2	1.2±0.3
	M-85	2–5	99.4±0.6	0.4±0.0	−0.5±0.1	0.2±0.1	0.4±0.2	
Phe[c]	M-57	1–9	22.8±0.4 (22.5)	42.7±0.7 (46.0)	26.0±0.4 (27.5)	3.8±0.2 (4.0)	0.1±0.1 (0.0)	1.5±0.5[b]
	M-85	2–9	24.4±0.6 (22.6)	44.9±1.1 (46.0)	28.1±1.3 (27.4)	4.0±0.2 (4.0)	−1.6±2.6 (0.0)	−0.0±0.2[b]
	f302	1–2	98.1±0.3 (98.2)	1.8±0.1 (1.8)	0.1±0.1 (0.0)			
Pro[b]	M-159	2–5	99.1±1.1	0.2±0.0	0.4±0.2	0.2±0.2	0.2±0.4	
Ser	M-57	1–3	54.4±5.4 (50.3)	45.5±0.8 (48.6)	0.1±0.1 (1.1)	2.3±0.1[b]		
	M-85	2–3	53.2±1.2 (51.0)	46.7±1.2 (48.4)	0.1±0.1 (0.5)			
	M-159	2–3	53.9±0.9 (51.0)	45.0±0.8 (48.4)	1.1±0.1 (0.5)			
	f302	1–2	98.5±0.1 (98.8)	1.2±0.0 (1.2)	0.3±0.1 (0.0)			
Thr	M-57	1–4	52.5±0.5 (51.8)	47.7±0.3 (48.0)	−0.0±0.2 (0.2)	−0.1±0.2[b]	−0.0±0.0[b]	
	M-85	2–4	50.9±0.3 (52.0)	47.3±0.4 (47.9)	1.0±0.2 (0.1)	0.8±0.2[b]		
Val	M-57	1–5	26.1±0.2 (27.1)	48.1±0.8 (49.9)	24.8±0.1 (23.0)	1.3±0.2[b]	0.0±0.1[b]	−0.2±0.3[b]
	M-159	2–5	26.6±0.6 (27.2)	46.8±1.7 (49.9)	22.4±1.0 (22.9)	3.7±3.0[b]	0.5±0.3[b]	
Fum	M-57	1–4	51.5±1.0 (51.8)	50.1±0.6 (48.0)	−0.7±0.5 (0.2)	−0.9±0.5[b]	0.1±0.4[b]	
Suc	M-15	1–4	50.7±0.2 (51.8)	49.2±0.2 (48.0)	0.1±0.0 (0.2)	0.0±0.0[b]	−0.0±0.0[b]	
	M-57	1–4	51.1±0.4 (51.8)	49.8±0.2 (48.0)	−0.1±0.5 (0.2)	−0.1±0.2[b]	−0.7±0.3[b]	

[a]Negative values are the result of correcting for natural abundances and can be treated as having zero value. The distributions shown were corrected as described in the methods and also for natural ^{13}C abundance in the amino and organic acid backbones using an excel macro developed by Joerg Schwender (Brookhaven National Laboratory, Upton, NY) based on correction matrices described by Lee et al. (1991). Simulated values resulting from the optimized set of fluxes (i.e., Fig. 3 fluxes) are in parentheses.
[b]Values were omitted from the fitting procedure.
[c]Data for Phe's highest mass fragments were omitted from the table.

metabolic network (specified by the user) and an arbitrary set of starting values for the free fluxes to simulate a data set of isotopomers and extracellular fluxes. The simulated data set is then compared to the experimental data set, and the fit between simulated and experimental data is determined by a sum of squared residuals (SS_{res}) weighted by their respective standard deviations. The free flux values are then varied until the weighted SS_{res} is minimized, indicating an optimized fit between the two data sets. The choice of free flux starting values can affect the resulting SS_{res} value if local minima are encountered in the optimization process. We used thousands of starting values to determine if multiple solutions existed. This process was automated using a Perl script, 'autoflux3.pl,' written by Hart Poskar (University of Manitoba, Canada). Natural ^{13}C abundance in the supplied glucose was included in the model. Mass distribution data were therefore corrected only for natural isotope abundances in all TBDMS atoms and all amino acid heteroatoms, and for unlabeled inoculum biomass, using software described by Wahl et al. (2004). The heaviest mass isotopomers were omitted from the fitting process, since their occurrence is highly improbable when starting from a singly-labeled isotopomer (Table 2) and they are therefore likely to be overestimated due to contaminants. NMR alanine and glycogen data were corrected for the inoculum's unlabeled biomass as described (Fischer and Sauer, 2003).

2.8. Analytical techniques for determining *A. succinogenes* cellular composition

A. succinogenes was grown as described above and harvested at 0.6–2.1 OD_{660}. Samples were centrifuged and washed at least once in 0.9% NaCl at 4 °C prior to analysis,

except for dry cell weight determination. All sample measurements were compared to the corresponding OD_{660} values by linear regression.

Dry cell weight was determined from thirteen cell suspensions, each composed of 3–5 pooled cultures. Suspensions were filtered through pre-weighed 0.45 μm HA filters (Millipore, Billerica, MA) and washed with 10 ml of 0.9% NaCl or water. The biomass-containing filters were dried to constant weight at 85 °C for 24 h, and the weights recorded.

Total protein and RNA contents were determined from 12 cultures each. For protein content, cell pellets from 1-ml culture samples were resuspended in 0.5 ml water, lysed by sonication, and lysate protein (20 μl) was quantified by the bicinchoninic acid assay (Pierce) with bovine serum albumin as the standard (McKinlay and Zeikus, 2004). Total cell RNA quantification was based on the method of Benthin et al. (1991). Cell pellets from 9-ml culture samples were resuspended in 3 ml of 0.3 M KOH and digested for 1 h at 37 °C, then chilled on ice. Ice-cold 3 M $HClO_4$ (1 ml) was added to the suspension, then $KClO_4$ and insoluble cell components were pelleted by centrifugation. The supernatant was saved, and RNA was extracted from the pellet twice more with 4 ml of ice-cold 0.5 M $HClO_4$. The supernatants were pooled and brought up to 13 ml with 0.5 M $HClO_4$. Samples were neutralized with 2 M Tris-HCl (pH 7.4) and the absorbance was measured at 260 and 280 nm (A_{260}:A_{280} ratios were between 1.9 and 2.0). A correspondence of 1.0 A_{260} to 40 mg RNA/l was used (Ausubel et al., 1998). The accuracy of the method was confirmed by performing the RNA and dry weight determinations on six *Escherichia coli* cultures grown aerobically in modified-M9 without casamino acids (McKinlay and Zeikus, 2004) and obtaining the expected RNA content of 20.8% of the dry cell weight (Neidhardt, 1987).

Total cell lipid was determined from six cultures using a transmethylation protocol (Li et al., 2006). Cell pellets were resuspended in 1 ml water and volumes containing ~25 mg of biomass were transferred to glass screw cap tubes and dried by lyophilization. Cells were resuspended in 2 ml of fresh 5% H_2SO_4 in methanol. To this solution were added 25 μl of 0.2% butylated hydroxy toluene in methanol and 24 μl of internal standard containing 1.74 mg/ml glyceryl triheptadecanoate in a 2:1 mixture of 2,2,4-trimethylpentane:toluene. The reaction mixtures were heated and quenched, and fatty acid methyl esters were extracted and analyzed by GC as described (Li et al., 2006). Peak identities were determined from fatty acid standards GLC-10 and GLC-50.

Total glycogen was determined from 18 cultures. Cell pellets from 6 to 10 ml of culture were resuspended in 1.4 ml of 50 mM sodium acetate buffer (pH 4.5) and lysed by sonication, followed by 5 min of boiling. Lysate samples (0.75 ml) were used to determine the initial glucose concentrations by HPLC. To ensure total glucose release, 6700 U of isoamylase and 3 U of amyloglucosidase were incubated with the lysates for 20–90 h at 40 °C with occasional mixing. At various time points, cell debris was pelleted by centrifugation and glucose in the supernatant was quantified by HPLC. Similar glucose yields were observed in 20 and 90 h digests. Isoamylase was required for complete digestion during this time, as determined by comparing glucose released from digests of type II glycogen from oyster with and without isoamylase (data not shown).

Peptidoglycan (PG) and lipopolysaccharide (LPS) levels were estimated from the difference in the surface area:-volume ratios of *A. succinogenes* and *E. coli*, using the same PG:LPS ratio for *A. succinogenes* as for *E. coli* (Neidhardt, 1987). The dimensions of 25 *A. succinogenes* and 43 *E. coli* exponential phase cells were measured by phase contrast microscopy. Volumes and surface areas were calculated assuming that each cell pole was a hemi-sphere and that the section between the hemi-spheres was a right cylinder.

To determine *A. succinogenes'* amino acid composition, lysates were prepared as described for total protein determination and centrifuged. Supernatants were dried by lyophilization, washed four times with ice-cold 80% ethanol in water to remove free amino acids, and dried under vacuum. Proteins were hydrolyzed under vacuum with 6 N HCl at 110 °C for 24 h. Amino acid analysis was performed at the MSU Macromolecular Structure Facility using a Hitachi L-8800 amino acid analyzer (San Jose, CA).

To determine the *A. succinogenes* C and N contents, cultures were harvested and washed three times with 0.9% NaCl. Pellets were resuspended in 1 ml water, boiled for 10 min, and dried by lyophilization. The C and N composition was then determined by the Duke Environmental Stable Isotope Laboratory, Duke University as described (Li et al., 2006).

2.9. Enzyme assays

Cell extracts were prepared from *A. succinogenes* grown in AM3. Cell pellets were washed in 0.9% NaCl, resuspended in 100 mM Tris-HCl (pH 7.4), and lysed by sonication. Soluble cell extracts were the supernatant of centrifuged lysate, whereas particulate cell extracts were not centrifuged. Cell extract protein was quantified using the bicinchoninic acid assay. All enzyme activities were measured in at least triplicate using a Cary 300 spectrophotometer (Varian, Palo Alto, CA) in final volumes of 1 ml at 37 °C. All reactions were started by adding the substrate, except for OAA decarboxylase, which was started by adding cell extract after the spontaneous OAA degradation rate was measured. Any background activity before adding the substrate was subtracted from the activity detected after adding the substrate. Extinction coefficients ($mM^{-1}\,cm^{-1}$) used were: 3-acetylpyridine adenine dinucleotide, 6.1 (Venning and Jackson, 1999); benzyl viologen (BV), 8.65; OAA, 0.95; NAD^+ and $NADP^+$, 6.23.

Formate dehydrogenase was assayed by monitoring BV reduction at 578 nm or NAD^+ reduction at 340 nm in a mixture containing 100 mM Tris-HCl (pH 7.4), 2 mM BV or NAD^+, 5 mM sodium formate, and 0.2 mg/ml particulate cell extract protein. The reaction was made anoxic by flushing solutions with N_2 for 10 min, sealing cuvettes with rubber stoppers, and injecting the substrate through the stopper. Malic enzyme was assayed by monitoring $NADP^+$ reduction at 340 nm in a mixture containing 75 mM Tris-HCl (pH 8.1), 4 mM $MnCl_2$, 1 mM dithiothreitol, 1 mM $NADP^+$, 40 mM disodium malate, 20 μg/ml soluble cell extract protein, and in the presence or absence of 2 mM NH_4Cl. To confirm that NH_4Cl did not activate other NADPH-producing activities, reactions were stopped by cooling on ice, then products were analyzed by HPLC. OAA decarboxylase was assayed by monitoring OAA removal at 265 nm (Dimroth, 1981) in a mixture containing 75 mM Tris-HCl (pH 7.4), 1 mM potassium OAA, 85 μg/ml particulate or 20 μg/ml soluble cell extract protein, in the presence or absence of 15 mM NaCl. OAA decarboxylation to pyruvate was confirmed by analyzing the reaction products by HPLC. Pyruvate dehydrogenase was assayed as described (Millar et al., 1998) in a mixture containing 750 μg/ml soluble cell extract protein. Transhydrogenase was assayed as described (Sauer et al., 2004) in a mixture containing 170 μg/ml particulate cell extract protein.

3. Results

3.1. Determining A. succinogenes' cellular composition

Knowing the requirements for metabolic intermediates used for biosynthesis is essential for accurately quantifying metabolic fluxes and for estimating ATP and redox balances. This knowledge can be obtained by quantifying cell components, or by assuming a cell composition similar to that of *E. coli*, and relating the values to central metabolism through anabolic pathway stoichiometries (Henriksen et al., 1996; Ingraham et al., 1983; Lange and Heijnen, 2001; Marx et al., 1996; Sauer et al., 1996). We determined the *A. succinogenes* glycogen, lipid, protein, and RNA levels, which together account for ~86% of the dry cell weight. At an OD_{660} of 1.0 in AM3, *A. succinogenes* had a concentration of 535 ± 47 mg dry cell wt/l. *A. succinogenes* amino acid and fatty acid compositions were also determined (Table 1). DNA levels were estimated by assuming the same genome copy number for *A. succinogenes* as for *E. coli* and adjusting for cells per gram of dry biomass (*A. succinogenes*, 3.3×10^{15}; *E. coli*, 1.1×10^{15} [Neidhardt, 1987]) and for genome sizes (*A. succinogenes*, 2.1 Mb; *E. coli* K12, 4.6 Mb). LPS and PG were estimated from the differences in surface area:volume ratios between *A. succinogenes* and *E. coli*. With cell dimensions of $0.63 \times 0.63 \times 1.21$ μm (*A. succinogenes*) and $0.80 \times 0.80 \times 2.63$ μm (*E. coli*), *A. succinogenes* has a surface area:volume ratio 1.39 times that of *E. coli*. Table 1 summarizes *A. succinogenes*' cell composition and its metabolite and cofactor requirements.

3.2. Confirming a pseudo-metabolic steady state

Since industrial fermentations typically occur as batch processes, we decided to perform flux analysis with *A. succinogenes* under batch conditions. Fig. 2 shows batch *A. succinogenes* growth and fermentation characteristics in AM3, during which the pH decreases from 7.2 to 6.4. Metabolic flux analysis uses equations that describe a metabolic steady state, where the fluxes into a metabolite pool equal the fluxes out of that pool. In batch cultures, however, changing cell, substrate, product, and proton concentrations can potentially affect metabolic fluxes. To confirm that *A. succinogenes* fluxes were constant during exponential growth, we first grew 11-ml cultures with unlabeled glucose and compared extracellular fluxes (specific rates of glucose consumption and product formations) at different cell densities in duplicate (i.e., at OD_{660} values of 0.5, 1.0, and 1.5) as described in the methods. The pH at the highest cell concentration sampled had only decreased to 7.0, and fermentation balances are known to be similar at pH values between 6.0 and 7.4 (van der Werf et al., 1997). The extracellular fluxes were similar at all cell densities (data not shown), so the experiment was repeated with nine cultures grown on [1-^{13}C]glucose as described in the Methods section. Extracellular fluxes and positional isotopic enrichments were compared in the cultures harvested at the different cell densities using Student's *t*-tests (95% confidence, equal-variance). A statistical difference occurred about once in every 19 comparisons,

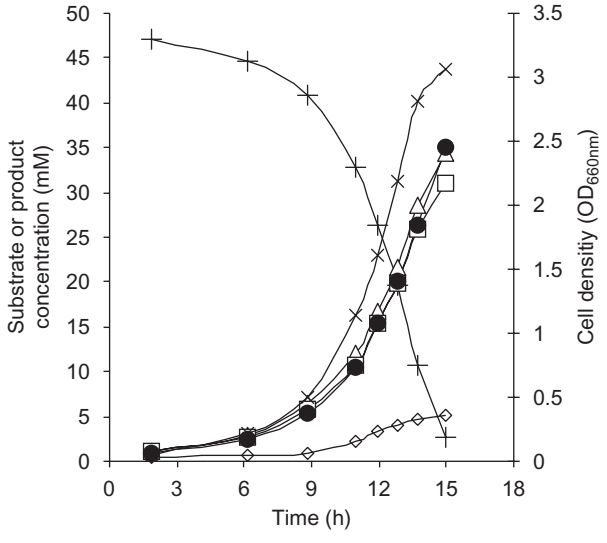

Fig. 2. *A. succinogenes* batch fermentation characteristics in AM3. Data were obtained from triplicate 60-ml cultures rather than 11-ml cultures to avoid significant volume changes during the course of the fermentation. Data obtained from parallel 11-ml cultures sampled showed nearly identical fermentation characteristics (data not shown). Standard deviations are less than or equal to the size of the symbols. Legend: glucose, +; succinate, ●; formate, △; acetate, □; ethanol, ◇; growth, ×.

which is indistinguishable from the expected frequency for false positive occurrences. Based on these results we felt confident that our batch cultures exhibited a pseudo-metabolic steady state during exponential growth, and we averaged the data across all nine cultures for use in our metabolic flux analysis.

3.3. Metabolic pathway delineation and flux quantification

To better understand *A. succinogenes* in vivo pathway utilization we used our biomass (Table 1), extracellular flux (Table 3), and isotopomer data sets (Tables 2 and 4) in several variations of the metabolic model shown in Fig. 1. This process was done both manually and by using ^{13}C-*Flux* software. Where possible, the values used were the average from all nine cultures, sampled at different cell densities. The set of fluxes giving the best fit between the simulated and experimental data sets (weighted $SS_{res} = 148$) is shown in Fig. 3. This model contains 28 free net fluxes and 11 free exchange fluxes (39 degrees of freedom). With a $SS_{res} > 54$, our fitting fails the χ^2 test at the 95% confidence interval, but this result is observed with most flux analysis studies of biological systems (Wiechert and de Graaf, 1997).

Non-oxidative PPP models usually consist of three reactions (ppp1-3; Fig. 1). Additional reactions may exist, though, that can affect the resulting global flux values. We tested the effects of including additional PPP reactions (van Winden et al., 2001) and of describing all possible PPP reactions as a simplified set of half reactions (Kleijn et al., 2005). These models gave nearly identical fluxes and weighted SS_{res} values (152 when including additional reactions and 154 when using half-reactions) as when only traditional PPP reactions were included. Because alternative PPP reactions have not been solidly established in vivo, and because they did not affect the resulting fluxes, we did not use alternative PPP reactions in our final model.

Our focus was to identify pathways involved in distributing flux to succinate and alternative fermentation products as well as those involved in redox balance. For this reason, and because the ATP required for cell maintenance is unknown, we did not focus on why the net ATP production is 1.6 times greater than the estimated requirement. Fig. 3 is described in detail below, focusing on the pathways of interest, and explaining the progression from the metabolic model shown in Fig. 1 to that shown in Fig. 3.

3.4. The glyoxylate cycle

The glyoxylate cycle could act as a shunt between the C_3 and C_4 pathways. Because low in vitro isocitrate lyase activity was reported for *A. succinogenes* (van der Werf et al., 1997), we investigated the presence of a functioning glyoxylate cycle in our ^{13}C-labeling experiment. Glyoxylate shunt flux was first addressed by inspection of the isotopomer data. As seen in Fig. 4, the [3-^{13}C]OAA and [2-^{13}C]acetyl-CoA produced from [1-^{13}C]glucose would generate double-labeled OAA through an active glyoxylate cycle. Table 2 shows insignificant fractions of double-labeled OAA-derived products (i.e., Asp, Thr, Fum, and Suc). These results suggest that the glyoxylate cycle, if present in *A. succinogenes*, is not active in cultures grown in AM3. Confirming our manual inspection of the data, all fittings of simulated to experimental data in ^{13}C-*Flux* indicated no forward or reverse glyoxylate cycle flux. These results agree with the fact that no *Pasteurellaceae* genome sequenced to date (complete or incomplete) contains genes showing similarity to known malate synthase and isocitrate lyase genes.

Table 4
Measured and simulated percent ^{13}C-enrichments in alanine, glucose, and organic acids as determined by NMR

Compound/Carbon	^{13}C enrichment (%)[a]	
	^{1}H-NMR	^{13}C-NMR
Acetate/C1	5.1±0.5 (4.7)[b]	4.9±0.8 (4.7)
Acetate/C2	42.5±1.0 (43.1)	42.5±1.0 (43.1)[d]
Alanine/C2	4.9±0.4 (4.7)[b,c]	5.4±0.7 (4.7)
Alanine/C3	43.9±0.9 (43.1)[c]	43.9±0.9 (43.1)[d]
Formate	0.0±0.0 (0.3)	N.D.
Glucose/C1	97.6±3.3 (97.2)	97.6±3.3 (97.2)[d]
Glucose/C6	N.D.	1.3±0.2 (1.4)
Succinate/C1 or C4	N.D.	0.0±0.0 (0.3)
Succinate/C2 or C3	24.0±0.2 (23.9)	24.0±0.2 (23.9)[d]

[a]Simulated values resulting from the optimized set of fluxes (i.e., Fig. 3 fluxes) are in parentheses.

[b]Long range coupling between ^{1}H and neighboring ^{13}C (i.e., acetate, $^{2}J^{1}H^{\alpha}$-^{13}C; alanine, $^{2}J^{1}H^{\beta}$-$^{13}C^{\alpha}$).

[c]While there is considerable overlapping of peaks in the ^{1}H-NMR spectra of amino acids, the peaks representing the alanine C^3 protons are sufficiently resolved for accurate quantification.

[d]Since ^{13}C-NMR only gives relative peak intensities, the ^{1}H-NMR-determined value for this carbon was used to represent the ^{13}C-NMR peak area. The label represented by ^{13}C-NMR peaks for other carbons was then determined from the relative peak intensity.

Table 3
Growth and metabolic parameters

μ (h^{-1})	Specific rates (mmol g^{-1} h^{-1})						Carbon recovery (%)	Electron recovery (%)
	r_{Glc}	r_{Suc}	r_{Fum}	r_{For}	r_{Ace}	r_{EtOH}		
0.28±0.01	7.9±0.5	5.8±0.3	0.2±0.0	3.5±0.3	4.4±0.2	1.2±0.2	98±4	104±4

The carbon and electron recoveries were calculated using an assumed elemental composition of $CH_2O_{0.5}N_{0.2}$. This typical microbial composition (Stephanopoulos et al., 1998) agrees with the C:N ratio for *A. succinogenes* ($CN_{0.18}$).

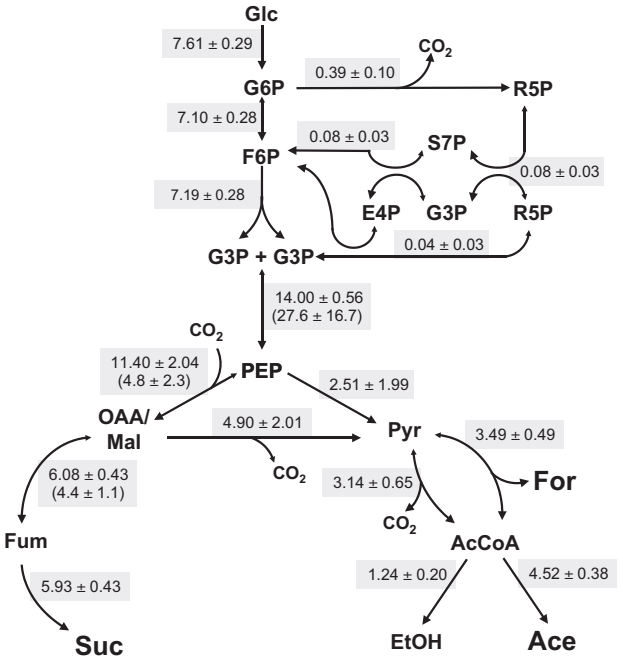

Additional net fluxes.

ATP	NADH	CO_2 uptake	Fum production
8.23	3.43	2.47 ± 0.92	0.15 ± 0.02

Net Anabolic fluxes.

G6P	F6P	R5P	E4P	G3P	PEP	Pyr	AcCoA	OAA
0.12	0.04	0.19	0.04	0.42	0.10	0.78	0.86	0.42

Fig. 3. *A. succinogenes* metabolic fluxes in AM3 with 150 mM $NaHCO_3$ obtained after fitting of experimental and simulated data sets in ^{13}C-*Flux*. All flux values have units of mmol g^{-1} h^{-1}. Single parameter 90% confidence intervals were calculated as described (Wiechert et al., 1997). Net flux directions are indicated by an enlarged arrowhead. Exchange flux values are in parentheses. Exchange fluxes that could not be quantified are indicated by a bi-directional arrow without an exchange flux value. Anabolic fluxes are based on Table 1 values. Anabolic flux requirements for 3-phosphoglycerate, Tyr, and Trp are accounted for in other anabolic fluxes. The estimated ATP, NADH, and NADPH fluxes for biosynthesis and transport were −13.36, 0.78, and −3.83, respectively. Reversible citrate lyase was omitted because there was no glyoxylate shunt flux and citrate was not observed in culture supernatants.

3.5. The oxidative pentose phosphate pathway

Since succinate production from PEP requires reductant (Fig. 1), it is important to understand *A. succinogenes*' redox balance. The OPPP was thought to be important for NADPH production based on previous enzyme activity data (van der Werf et al., 1997). Also, the *A. succinogenes* genome sequence encodes the OPPP enzymes, glucose-6-phosphate (G6P) dehydrogenase (AsucDRAFT_0146) and 6-phosphogluconate dehydrogenase (AsucDRAFT_0141). We first addressed OPPP flux by inspecting the isotopomer data. While glycolysis converts [1-^{13}C]G6P into equal proportions of unlabeled and single-labeled G3P, the OPPP produces $^{13}CO_2$ and unlabeled G3P (Fig. 5a). Between 45.5% (in Ser) and 50.1% (in Fum) of each downstream product of G3P (i.e., Ala, Asp, Fum, Ser, Suc,

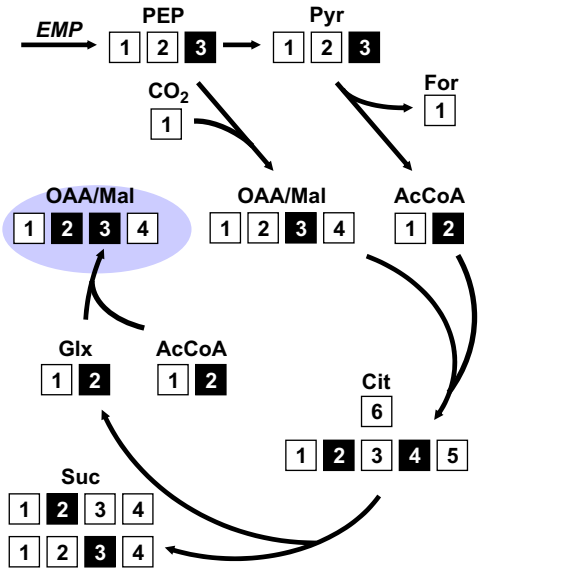

Fig. 4. Acetyl-CoA and OAA isotopomers expected from forward glyoxylate cycle flux. Black squares, ^{13}C; white squares, ^{12}C. The shaded oval highlights the double-labeled OAA that would be generated by glyoxylate cycle flux.

and Thr) contain a single label (Table 2). These values are close to the 50% expected from glycolytic flux alone. However, to accurately quantify the glycolytic and OPPP fluxes, the existence of [6-^{13}C]G6P should be considered. [6-^{13}C]G6P is produced by reverse flux from [6-^{13}C]fructose-6-phosphate, which is generated by triose-phosphate cycling (Schwender et al., 2003) and reverse PPP reactions. NMR analysis of glycogen's glucose monomers shows that only 1.4% of G6P is labeled at carbon 6 (Table 4), indicating very little OPPP flux.

We then used ^{13}C-*Flux* to quantify the OPPP flux. Since there is a net CO_2 consumption by *A. succinogenes* fermentations, we originally only included a CO_2 influx in our model. This first model did not account for the possibility of $^{13}CO_2$ produced by the OPPP being diluted by the large amount of $^{12}CO_2$ in the medium. Without a CO_2 efflux, all fittings indicated no OPPP flux. Since most metabolites, with the exception of fumarate and succinate, indicate a small ^{13}C loss from the system (Tables 2 and 4), we included a CO_2 efflux in the model. The OPPP flux was 5% that of the glucose uptake rate, only enough to supply 20% of the estimated NADPH requirements (Fig. 3).

Like OPPP flux, Cys and Met uptake would contribute to unlabeled isotopomers. However, the fitting shown in Fig. 3 indicates no Cys and Met uptake. To determine if our adjustment of the mass isotopomer standard deviations (see Methods) prevented the detection of Cys and Met uptake, we used unmodified standard deviations in the fitting process. The best fit in this case (SS_{res} of 384) showed essentially the same set of fluxes, including no Met uptake and a very small Cys uptake (1% of the glucose uptake rate). As expected, OPPP flux was lower (4% of the glucose uptake rate) in the fit showing Cys uptake. If our model underestimates the extent of Cys and Met uptakes, then it

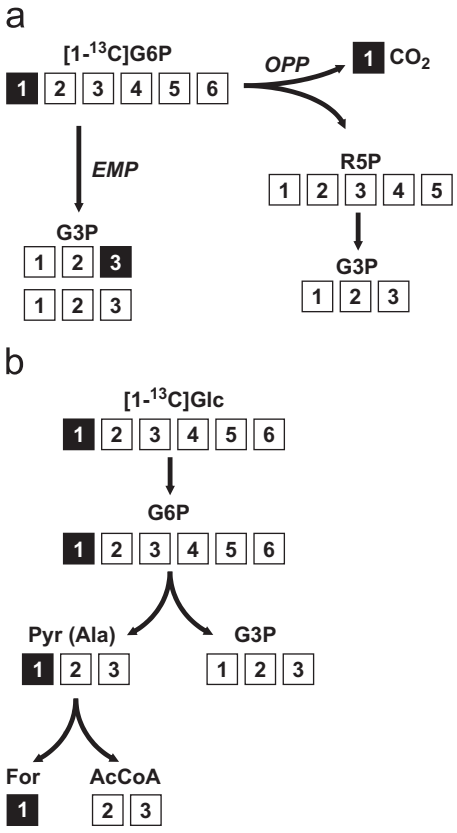

Fig. 5. Isotopomers expected from OPPP and ED pathway fluxes. Black squares, ^{13}C; white squares, ^{12}C. A. G3P isotopomers expected from forward glycolytic and OPPP fluxes. B. Alanine and formate isotopomers expected from ED pathway flux.

overestimates the OPPP flux as well. Thus, 20% represents the upper limit of the NADPH requirements that can be supplied by the OPPP.

3.6. The Entner–Doudoroff pathway

With low OPPP flux, other pathways must be responsible for NADPH production. Previously, low ED pathway enzyme activities were detected in *A. succinogenes* extracts (van der Werf et al., 1997). The *A. succinogenes* genome encodes two proteins showing 36% and 37% identity to *E. coli* 2-keto-3-deoxy-6-phosphogluconate aldolase (AsucDRAFT_0727 and 1070) and a protein that is 27% identical to *E. coli* phosphogluconate dehydratase (AsucDRAFT_0513). For these reasons, we investigated the presence of ED pathway flux in our labeling experiment. Flux through the ED pathway would produce [1-^{13}C]pyruvate, resulting in [1-^{13}C]Ala and ^{13}C-formate (Fig. 5b). As seen in Table 2, Ala M-57 fragments (containing carbons 1–3) and M-85 fragments (containing carbons 2 and 3) have almost identical mass isotopomer distributions. Since losing Ala carbon 1 does not affect the mass distribution, carbon 1 must be 100% unlabeled. Furthermore, no labeled formate was observed by ^{1}H-NMR (Table 4). These results indicate that there is negligible ED pathway flux. All ^{13}C-*Flux* fittings using models containing the ED pathway confirmed this conclusion.

3.7. C_3 pathway dehydrogenases and transhydrogenase

HPLC analysis of excreted products showed that 1.6 times more acetate + ethanol were excreted than formate. The expected ratio is <1.0 since pyruvate formate-lyase produces equal amounts of formate and acetyl-CoA (Fig. 1) and some acetyl-CoA is required for biomass (Fig. 3). This observation can be explained if formate dehydrogenase (ForDH) consumes some formate or pyruvate dehydrogenase (PyrDH) converts some pyruvate to acetyl-CoA and CO_2. The *A. succinogenes* genome encodes both PyrDH (AsucDRAFT_001-003) and ForDH (AsucDRAFT_1405-1408), and in vitro activity was detected for both enzymes (Table 5). ForDH is often coupled to hydrogenase in bacterial fermentations, producing H_2 rather than NADH. Here, the electron balance was $104\pm4\%$ (Table 3) and GC analysis showed that H_2 was absent from culture headspaces, indicating either that H_2 was not produced or that it was quickly consumed. In any case, pyruvate oxidation to acetyl-CoA without formate or H_2 production yields reductant. Our metabolic flux model (Fig. 3) indicates a $3.14\,mmol\,g^{-1}\,h^{-1}$ flux through the PyrDH/ForDH grouped reaction, giving a total NADH production rate of $17.92\,mmol\,g^{-1}\,h^{-1}$ (including NADH produced by G3P dehydrogenase and anabolism). Succinate and ethanol productions require a total of $14.49\,mmol\,NADH\,g^{-1}\,h^{-1}$ (Fig. 3), leaving $3.43\,mmol\,NADH\,g^{-1}\,h^{-1}$ to be consumed by other reactions. One possibility for an NADH-consuming reaction is transhydrogenase. The *A. succinogenes* genome encodes a membrane-associated transhydrogenase (AsucDRAFT_0847-848). In vitro transhydrogenase activity was previously reported as diaphorase activity (Park and Zeikus, 1999), and it was also detected in this study (Table 5). If the excess

Table 5
Enzyme activities in cell extracts of *A. succinogenes* grown in AM3 with 150 mM $NaHCO_3$

Enzyme assayed	Specific activity ($nmol\,mg\,protein^{-1}\,min^{-1}$)
Transhydrogenase	14 ± 1
Pyruvate dehydrogenase	5 ± 1
Formate dehydrogenase[a]	7 ± 2
Malic enzyme ($-\ NH_4^+$)[b]	120 ± 10
Malic enzyme ($+\ NH_4^+$)[b]	620 ± 50
Soluble OAA decarboxylase ($-\ Na^+$)[c]	260 ± 60
Soluble OAA decarboxylase ($+\ Na^+$)[c]	80 ± 110
Particulate OAA decarboxylase ($+\ Na^+$)[c]	1080 ± 110

[a]Activity was not detected when NAD^+ was supplied in place of BV.
[b]Since NH_4^+ is known to stimulate malic enzyme activity (Sanwal and Smando, 1969), NH_4Cl was added to the reaction to confirm that the measured activity was due to malic enzyme. The amount of NADPH produced was $94\pm3\%$ that of the pyruvate produced.
[c]HPLC analysis confirmed that pyruvate was the main product formed.

NADH is consumed entirely by transhydrogenase, it could supply 90% of the estimated NADPH requirements.

3.8. Malic enzyme and OAA decarboxylase

While transhydrogenase and OPPP fluxes could account for up to 110% of the estimated NADPH requirements, other NADH-consuming (i.e., malate dehydrogenase) and NADPH-producing (i.e., malic enzyme) reactions are possible. Together, the reactions catalyzed by malate dehydrogenase and malic enzyme are an alternative to transhydrogenase, resulting in the net oxidization of NADH and reduction of $NADP^+$ (Fig. 1). Besides producing NADPH, malic enzyme also bridges the C_4 and the C_3 pathways (Fig. 1). Therefore, the existence of a malic enzyme flux could dramatically influence metabolic engineering strategies. Malic enzyme activity was detected in extracts of *A. succinogenes* grown in several conditions (van der Werf et al., 1997), including in AM3 (Table 5). To distinguish fluxes between PEP and pyruvate from fluxes between OAA/malate and pyruvate, a unique isotopomer of pyruvate or OAA/malate must be present. As illustrated in Fig. 6, a unique isotopomer, [2-^{13}C]fumarate, is formed when scrambling caused by the symmetry of fumarate generates 25% each of [3-^{13}C]fumarate and [2-^{13}C]fumarate (50% of the fumarate is unlabeled). Exchange flux in the C_4 pathway then generates 7% [2-^{13}C]OAA and 2% [2-^{13}C]PEP (determined from GC-MS analyses of Asp's and Phe's f302 fragments, respectively; Table 2). If all pyruvate were generated from PEP, as would be expected in a simple branched fermentation, pyruvate and PEP would have identical positional isotopic enrichments. NMR analyses of Ala (Table 4) show that 5%, rather than 2%, of pyruvate is labeled at the C2 position. This result indicates that a C_4-decarboxylating enzyme (i.e., malic enzyme or OAA decarboxylase) is active during growth in AM3. This conclusion is also supported by the detection of 5% [1-^{13}C]acetate (Table 4), a downstream product of [2-^{13}C]pyruvate.

Because fluxes from OAA, malate, and PEP to pyruvate give identical pyruvate isotopomers, and because different combinations of these three fluxes can result in identical pyruvate isotopomer distributions, OAA and malate decarboxylating fluxes cannot be distinguished. For this reason, malate and OAA were grouped into a single pool, as in other metabolic flux models (Christensen and Nielsen, 2000; Marx et al., 1996; Petersen et al., 2000; Wendisch et al., 2000; Wittmann and Heinzle, 2001). In Fig. 3, PEPCK and PK net flux values were dependent on the OAAdec/ME flux (set as a free variable), explaining why PEPCK, PK, and OAAdec/ME fluxes have similar confidence intervals. These confidence intervals are large, and different values for fluxes between PEP, OAA/malate, and pyruvate were obtained in multiple fittings with little effect on the SS_{res} value. However, our fittings consistently showed that the OAAdec/ME flux was larger than the PK flux. The best fit indicates that the C_4-decarboxylating flux is

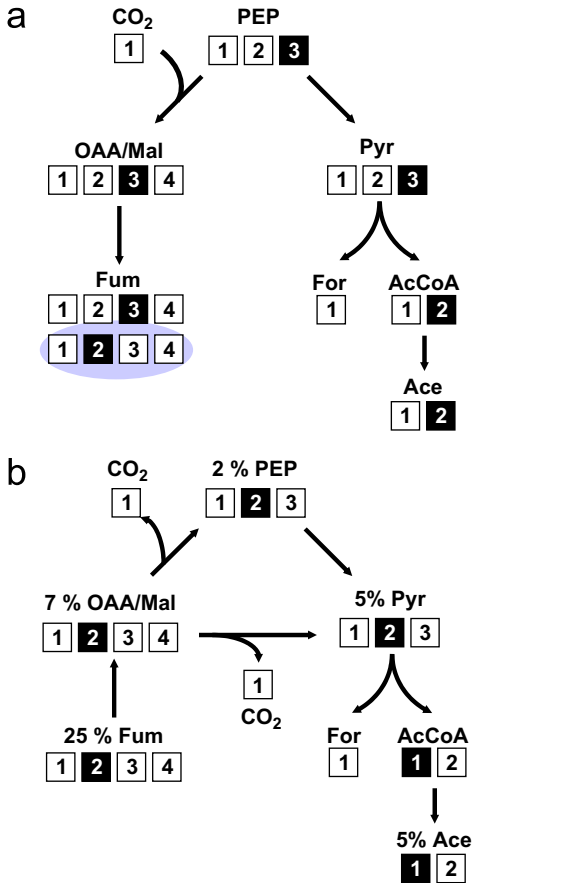

Fig. 6. Two-step illustration of the fluxes resulting in [2-^{13}C]pyruvate. Black squares, ^{13}C; white squares, ^{12}C. (A) Step 1: Generation of [2-^{13}C]fumarate (highlighted by the shaded oval) by forward fluxes through the C_4 pathway and fumarate's symmetry. (B) Step 2: Isotopomers resulting from [2-^{13}C]fumarate by reverse C_4 pathway flux, C_4-decarboxylating flux, and forward C_3 pathway flux.

4.9 mmol g^{-1} h^{-1}, which is greater than the flux needed to convert excess NADH to NADPH (3.43 mmol g^{-1} h^{-1}). Therefore, the C_4-decarboxylating flux must represent a combination of malic enzyme and OAA-decarboxylating fluxes, since OAA decarboxylation to pyruvate does not yield reductant. An operon encoding a membrane-bound, Na^+-pumping OAA decarboxylase was identified in the genome sequence (AsucDRAFT_1557-1559). In addition to detecting a Na^+-independent OAA decarboxylase activity in soluble cell extracts, we also detected significant Na^+-dependent activity in particulate cell extracts but not in soluble cell extracts (Table 5). From the flux analysis and enzyme activities detected, it is clear that flux distribution to succinate and alternative products can occur at OAA and malate, rather than just at PEP.

4. Discussion

This study has described important aspects of *A. succinogenes* metabolism. Flux through the glyoxylate and ED pathways was ruled out. OPPP flux was too low to meet NADPH requirements. PyrDH and/or ForDH

contribute to a net NADH production that could be converted to NADPH by transhydrogenase. Malic enzyme may also contribute to NADPH production. In addition to PEP, OAA and malate are important nodes for flux distribution to succinate and alternative fermentation products.

We assume that the excess ATP not needed for biosynthesis and transport (Table 1) is used for cell maintenance. The estimated ATP required for biosynthesis alone ($10.48\,mmol\,g^{-1}\,h^{-1}$) is 49% of the total ATP produced, which is not unreasonable. It was estimated that 51% of the energy produced by anaerobically growing *E. coli* is used for transport and maintenance processes (Stouthamer, 1979).

Optimized fits showed a greater OAAdec/ME flux than PK flux. PK flux is composed of pyruvate kinase and the PTS. If glucose phosphorylation occurred through the PTS alone, the PK flux would be at least equal to the glucose uptake rate. Because the estimated PK flux is only 33% of the glucose uptake rate, and because most of the flux into the C_3 pathway is likely from OAA/malate rather than from PEP (Fig. 3), it is unlikely that the PTS is the main glucose phosphorylation mechanism. *A. succinogenes* was previously shown to have hexokinase activity in addition to PTS activity (van der Werf et al., 1997). Uptake assays with ^{14}C-glucose and a ^{14}C-glucose analogue indicated that the PTS is not the main *A. succinogenes* glucose uptake mechanism at high glucose concentrations (Kim and Vieille, submitted).

This study identified the mechanisms responsible for NADPH production in glucose-grown *A. succinogenes* in AM3. Product isotopomer data indicated no ED pathway flux and low OPPP flux. The lower flux to formate than to acetyl-CoA indicated, in addition to pyruvate formate-lyase activity, a pyruvate oxidizing activity (i.e., PyrDH) and/or a formate oxidizing activity (i.e., ForDH). PyrDH is often considered to be an enzyme of aerobic metabolism. However, it is expressed in anaerobically grown *Haemophilus influenzae* (Raghunathan et al., 2004), a bacterium closely related to *A. succinogenes*. PyrDH and ForDH activities were also detected in *A. succinogenes* cell extracts (Table 5). In either case, there is enough excess NADH to meet the NADPH requirements through transhydrogenase and/or through NADH-oxidizing malate dehydrogenase plus NADP-reducing malic enzyme. Product isotopomer data confirmed the existence of a C_4-decarboxylating flux, suggesting that malic enzyme contributes to NADPH production. NADP-dependent malic enzyme and transhydrogenase activities were detected in cell extracts (Table 5). Given the low OPPP flux, transhydrogenase and/or malic enzyme are the main NADPH-producing mechanisms, and account for at least 80% of the NADPH requirements.

Malic enzyme's contribution to NADPH production in *A. succinogenes* and other bacteria is currently unclear. Under ammonia-limiting conditions, or when pyruvate kinase is knocked out, malic enzyme flux increases in *E. coli*, but this results in excess NADPH that is oxidized by transhydrogenase (Emmerling et al., 2002). Transhydrogenase, on the other hand, is a significant NADPH producer in several cases. In fact, *E. coli* was recently shown to rely on transhydrogenase for up to 45% of its NADPH requirements in aerobic batch cultures (Sauer et al., 2004). Transhydrogenase is even more important for *E. coli* NADPH production when the OPPP enzyme, G6P dehydrogenase, is disrupted (Hua et al., 2003; Sauer et al., 2004). Transhydrogenase is also important for NADPH production in *Rhodospirillum rubrum* and *Rhodobacter sphaeroides* (Grammel et al., 2003; Hickman et al., 2002), suggesting an important role for this enzyme across a diverse range of bacteria. While we have shown that transhydrogenase and/or malic enzyme are important for NADPH production in *A. succinogenes*, it remains to be seen how flux through these enzymes and through the OPPP respond to environmental stimuli.

Understanding the NADPH-producing mechanisms in *A. succinogenes* may also be important for devising metabolic engineering strategies. It is well known that the CO_2 concentration affects the flux distribution into the C_4 and C_3 pathways (McKinlay et al., 2005; van der Werf et al., 1997). Here we have shown that flux to the C_3 pathway (i.e., malic enzyme) and flux through the C_3 pathway (i.e., PyrDH and ForDH) are important for NADPH production. Therefore, it is plausible that the need for NADPH also controls flux distribution between the C_4 and C_3 pathways. Under the conditions studied here, a limited quantity of reductant must be shared by the C_4 pathway and anabolism. Adding H_2 shifts the *A. succinogenes* fermentation balance toward succinate in rich media (van der Werf et al., 1997). Adding H_2 also, at least partially, alleviates the need for flux through C_3 pathway dehydrogenases, as shown by the fact that adding H_2 increases the formate:(acetate + ethanol) ratio in AM3-grown cultures (McKinlay et al., unpublished data). It will be important to determine whether a surplus of electrons (e.g., as H_2) will be sufficient to suppress the C_3 pathway or if genetic modifications are necessary.

The discovery of an in vivo C_4-decarboxylating flux is particularly important because it reveals that flux distribution to succinate and alternative products can occur at multiple nodes (i.e., PEP, OAA, malate, and possibly pyruvate). This discovery also implicates PEPCK as a major flux-carrying enzyme that feeds both product-forming branches rather than just the C_4 pathway. Thus, at least under the growth conditions tested here, OAA and malate could be more important nodes than PEP in controlling flux distribution to succinate and alternative products. There is currently much interest in the fields of bacterial physiology and metabolic engineering in understanding flux distribution at these nodes (Sauer and Eikmanns, 2005). In the case of *A. succinogenes,* it now seems likely that redirecting flux towards succinate production will face the engineering challenges of dealing with alternative routes (e.g., pyruvate kinase vs. PEPCK and a C_4-decarboxylase) and redundant activities. In this

study, malic enzyme and two OAA-decarboxylating activities were identified. The Na^+-dependent OAA decarboxylase activity was only observed in particulate cell extracts, which is consistent with the Na^+-pumping, membrane-bound OAA decarboxylase encoded in the *A. succinogenes* genome. Membrane-bound OAA decarboxylase is also expressed by closely related *Mannheimia succiniciproducens* grown anaerobically on glucose (Lee et al., 2006). While this enzyme is required for growth on citrate by other bacteria (Dahinden et al., 2005; Dimroth, 1980; Woehlke and Dimroth, 1994), its activity during glucose fermentation is an intriguing finding that suggests an alternative role. A role for OAA decarboxylase in Na^+-linked energetics has been suggested for several bacteria (Dimroth and Schink, 1998; Hase et al., 2001), including in Na^+-dependent glutamate transport and drug efflux in closely related *A. actinomycetemcomitans* (Hase et al., 2001). A Na^+ gradient could also be involved in fumarate and succinate transport as was shown for *Wolinella succinogenes* (Ullmann et al., 2000). However, given that AM3 contains ~230 mM Na^+, the membrane-bound OAA decarboxylase may simply function to pump Na^+ out of the cell. A Na^+-independent OAA-decarboxylating activity was detected in the soluble crude extract (Table 5). Malic enzyme (Sanwal and Smando, 1969), PEPCK (Jabalquinto et al., 1999), pyruvate kinase (Creighton and Rose, 1976), and 2-keto-3-deoxy-6-phosphogluconate aldolase (Patil and Dekker, 1992) can also decarboxylate OAA, at least in vitro. While the in vivo contribution of these OAA decarboxylating activities is unknown, the potential for redundant activities is considerable, and may present a challenge for metabolic engineering. On the other hand, a C_4-decarboxylating flux that only meets anabolic pyruvate and acetyl-CoA needs could be beneficial for developing a succinate-producing strain with an acceptable growth rate.

This study has provided key insights into *A. succinogenes* NADPH production and flux distribution to major fermentation products, and has raised important considerations for its metabolic engineering. ^{13}C-labeling studies of industrial organisms have not only led to strain improvements but also to a deeper understanding of metabolism. They have led to the discovery of new pathways (Christensen and Nielsen, 2000; Schwender et al., 2004), and to a better understanding of anaplerosis (Park et al., 1997; Petersen et al., 2000; Sauer and Eikmanns, 2005) and of the controls effected by cofactor production and cell energetics (Dauner et al., 2002; Sauer et al., 1997; Zamboni et al., 2003). The effects of CO_2 and alternative carbon and electron sources on *A. succinogenes*' fermentation balance make this bacterium an excellent system for analyzing the metabolic control effects of CO_2 and reducing power on flux distribution between PEP, pyruvate, OAA, and malate using ^{13}C-labeling and other studies. While *A. succinogenes* has industrial potential, it also has unique metabolic traits whose study could contribute to a broader understanding of bacterial metabolism and its diversity.

Acknowledgments

This work was supported by the National Science Foundation grant BES-0224596 and by a grant from the Michigan State University (MSU) Research Excellence Fund. James McKinlay was supported in part by MSU Quantitative Biology and Modeling Initiative and Marvin Hensley Endowed fellowships and by an Annie's Homegrown fellowship for environmental studies.

We are indebted to Dr. Douglas Allen for valuable discussions and technical assistance. We also thank Drs. John Ohlrogge, Ana Alonso, Fernando Goffman, Igor Libourel, and Joerg Schwender for valuable discussions. We are grateful for the use of Drs. Tom Schmidt's and John Ohlrogge's GC equipment. We are also grateful for the use of the autoflux3 program written by Dr. Hart Poskar. We thank Drs. Beverly Chamberlin, Daniel Holmes, and Joe Leykam for assistance with GC-MS, NMR, and amino acid analysis, respectively.

Appendix A. Supplementary Materials

Supplementary data associated with this article can be found in the online version at doi:10.1016/j.ymben.2006.10.006.

References

Ausubel, F.M., Brent, R., Kingston, R.E., Moore, D.D., Seidman, J.G., Smith, J.A., Struhl., K. (Eds.), 1998. Current Protocols in Molecular Biology. Wiley, New York.

Benthin, S., Nielsen, J., Villadsen, J., 1991. A simple and reliable method for the determination of cellular RNA content. Biotechnol. Tech. 5, 39–42.

Christensen, B., Nielsen, J., 2000. Metabolic network analysis of *Penicillium chrysogenum* using ^{13}C-labeled glucose. Biotechnol. Bioeng. 68, 652–659.

Creighton, D.J., Rose, I.A., 1976. Oxalacetate decarboxylase activity in muscle is due to pyruvate kinase. J. Biol. Chem. 251, 69–72.

Dahinden, P., Auchli, Y., Granjon, T., Taralczak, M., Wild, M., Dimroth, P., 2005. Oxaloacetate decarboxylase of *Vibrio cholerae*: purification, characterization, and expression of the genes in *E. coli*. Arch. Microbiol. 183, 121–129.

Dauner, M., Sauer, U., 2000. GC-MS analysis of amino acids rapidly provides rich information for isotopomer balancing. Biotechnol. Prog. 16, 642–649.

Dauner, M., Sonderegger, M., Hochuli, M., Szyperski, T., Wuthrich, K., Hohmann, H.P., Sauer, U., Bailey, J.E., 2002. Intracellular carbon fluxes in riboflavin-producing *Bacillus subtilis* during growth on two-carbon substrate mixtures. Appl. Environ. Microbiol. 68, 1760–1771.

Dimroth, P., 1980. A new sodium-transport system energized by the decarboxylation of oxaloacetate. FEBS Lett. 122, 234–236.

Dimroth, P., 1981. Characterization of a membrane-bound biotin-containing enzyme: oxaloacetate decarboxylase from *Klebsiella aerogenes*. Eur. J. Biochem. 115, 353–358.

Dimroth, P., Schink, B., 1998. Energy conservation in the decarboxylation of dicarboxylic acids by fermenting bacteria. Arch. Microbiol. 170, 69–77.

Emmerling, M., Dauner, M., Ponti, A., Fiaux, J., Hochuli, M., Szyperski, T., Wuthrich, K., Bailey, J.E., Sauer, U., 2002. Metabolic flux

responses to pyruvate kinase knockout in *E. coli*. J. Bacteriol. 184, 152–164.

Fell, D., 1997. Understanding the Control of Metabolism. Portland Press, London and Miami.

Fischer, E., Sauer, U., 2003. Metabolic flux profiling of *E. coli* mutants in central carbon metabolism using GC-MS. Eur. J. Biochem. 270, 880–891.

Grammel, H., Gilles, E.D., Ghosh, R., 2003. Microaerophilic cooperation of reductive and oxidative pathways allows maximal photosynthetic membrane biosynthesis in *Rhodospirillum rubrum*. Appl. Environ. Microbiol. 69, 6577–6586.

Guettler, M.V., Jain, M.K., Rumler, D., 1996a. Method for making succinic acid, bacterial variants for use in the process, and methods for obtaining variants. US Patent 5,573,931.

Guettler, M.V., Jain, M.K., Soni, B.K., 1996b. Process for making succinic acid, microorganisms for use in the process and methods of obtaining the microorganisms. US Patent 5,504,004.

Guettler, M.V., Rumler, D., Jain, M.K., 1999. *Actinobacillus succinogenes* sp. nov., a novel succinic-acid-producing strain from the bovine rumen. Int. J. Syst. Bacteriol. 49, 207–216.

Hase, C.C., Fedorova, N.D., Galperin, M.Y., Dibrov, P.A., 2001. Sodium ion cycle in bacterial pathogens: evidence from cross-genome comparisons. Microbiol. Mol. Biol. Rev. 65, 353–370.

Henriksen, C.M., Christensen, L.H., Nielsen, J., 1996. Growth energetics and metabolic fluxes in continuous cultures of *Penicillium chrysogenum*. J. Biotechnol. 45, 149–164.

Hickman, J.W., Barber, R.D., Skaar, E.P., Donohue, T.J., 2002. Link between the membrane-bound pyridine nucleotide transhydrogenase and glutathione-dependent processes in *Rhodobacter sphaeroides*. J. Bacteriol. 184, 400–409.

Hua, Q., Yang, C., Baba, T., Mori, H., Shimizu, K., 2003. Responses of the central metabolism in *E. coli* to phosphoglucose isomerase and glucose-6-phosphate dehydrogenase knockouts. J. Bacteriol. 185, 7053–7067.

Ingraham, J.L., Maaloe, O., Neidhardt, F.C., 1983. Growth of the Bacterial Cell. Sinauer Associates, Sunderland, MA.

Jabalquinto, A.M., Laivenieks, M., Zeikus, J.G., Cardemil, E., 1999. Characterization of the oxaloacetate decarboxylase and pyruvate kinase-like activities of *Saccharomyces cerevisiae* and *Anaerobiospirillum succiniciproducens* phosphoenolpyruvate carboxykinases. J. Protein. Chem. 18, 659–664.

Kim, P., Vieille, C., Glucose phosphorylation mechanisms in succinate-producing *Actinobacillus succinogenes*. submitted.

Kleijn, R.J., van Winden, W.A., van Gulik, W.M., Heijnen, J.J., 2005. Revisiting the ^{13}C-label distribution of the non-oxidative branch of the pentose phosphate pathway based upon kinetic and genetic evidence. FEBS J. 272, 4970–4982.

Koffas, M.A.G., Jung, G.Y., Stephanopoulos, G., 2003. Engineering metabolism and product formation in *Corynebacterium glutamicum* by coordinated gene overexpression. Metab. Eng. 5, 32–41.

Kroger, A., Biel, S., Simon, J., Gross, R., Unden, G., Lancaster, C.R.D., 2002. Fumarate respiration of *Wolinella succinogenes*: enzymology, energetics and coupling mechanism. Biochim. Biophys. Acta. 1553, 23–28.

Lange, H.C., Heijnen, J.J., 2001. Statistical reconciliation of the elemental and molecular biomass composition of *Saccharomyces cerevisiae*. Biotechnol. Bioeng. 75, 334–344.

Lee, J.W., Lee, S.Y., Song, H., Yoo, J.S., 2006. The proteome of *Mannheimia succiniciproducens*, a capnophilic rumen bacterium. Proteomics 6, 3550–3566.

Lee, W.N., Byerley, L.O., Bergner, E.A., Edmond, J., 1991. Mass isotopomer analysis: theoretical and practical considerations. Biol. Mass. Spectrom. 20, 451–458.

Li, Y., Beisson, F., Pollard, M., Ohlrogge, J., 2006. Oil content of *Arabidopsis* seeds: the influence of seed anatomy, light and plant-to-plant variation. Phytochemistry 67, 904–915.

Marx, A., de Graaf, A.A., Wiechert, W., Eggeling, L., Sahm, H., 1996. Determination of fluxes in the central metabolism of *Corynebacterium glutamicum* by nuclear magnetic resonance spectroscopy combined with metabolic balancing. Biotechnol. Bioeng. 49, 111–129.

McKinlay, J.B., Zeikus, J.G., 2004. Extracellular iron reduction is mediated in part by neutral red and hydrogenase in *E. coli*. Appl. Environ. Microbiol. 70, 3467–3474.

McKinlay, J.B., Zeikus, J.G., Vieille, C., 2005. Insights into *Actinobacillus succinogenes* fermentative metabolism in a chemically defined growth medium. Appl. Environ. Microbiol. 71, 6651–6656.

Millar, A.H., Knorpp, C., Leaver, C.J., Hill, S.A., 1998. Plant mitochondrial pyruvate dehydrogenase complex: purification and identification of catalytic components in potato. Biochem. J. 334, 571–576.

Neidhardt, F.C., 1987. *E. coli* and *Salmonella typhimurium* Cellular and Molecular Biology. American Society for Microbiology, Washington, DC.

Park, D.H., Zeikus, J.G., 1999. Utilization of electrically reduced neutral red by *Actinobacillus succinogenes*: physiological function of neutral red in membrane-driven fumarate reduction and energy conservation. J. Bacteriol. 181, 2403–2410.

Park, S.M., Shaw-Reid, C., Sinskey, A.J., Stephanopoulos, G., 1997. Elucidation of anaplerotic pathways in *Corynebacterium glutamicum* via ^{13}C-NMR spectroscopy and GC-MS. Appl. Microbiol. Biotechnol. 47, 430–440.

Patil, R.V., Dekker, E.E., 1992. Cloning, nucleotide sequence, overexpression, and inactivation of the *E. coli* 2-keto-4-hydroxyglutarate aldolase gene. J. Bacteriol. 174, 102–107.

Petersen, S., de Graaf, A.A., Eggeling, L., Mollney, M., Wiechert, W., Sahm, H., 2000. In vivo quantification of parallel and bidirectional fluxes in the anaplerosis of *Corynebacterium glutamicum*. J. Biol. Chem. 275, 35932–35941.

Raghunathan, A.N., Price, D., Galperin, M.Y., Makarova, K.S., Purvine, S., Picone, A.F., Cherny, T., Xie, T., Reilly, T.J., R.Munson, J., Tyler, R.E., Akerley, B.J., Smith, A.L., Palsson, B.O., Kolker, E., 2004. *In silico* metabolic model and protein expression of *Haemophilus influenzae* strain Rd KW20 in rich medium. Omics 8, 25–41.

Ratcliffe, R.G., Shachar-Hill, Y., 2006. Measuring multiple fluxes through plant metabolic networks. Plant J. 45, 490–511.

Sanwal, B.D., Smando, R., 1969. Malic enzyme of *E. coli*. Diversity of the effectors controlling enzyme activity. J. Biol. Chem. 244, 1817–1823.

Sauer, U., Eikmanns, B.J., 2005. The PEP-pyruvate-oxaloacetate node as the switch point for carbon flux distribution in bacteria. FEMS Microbiol. Rev. 29, 765–794.

Sauer, U., Hatzimanikatis, V., Hohmann, H.P., Manneberg, M., van Loon, A.P., Bailey, J.E., 1996. Physiology and metabolic fluxes of wild-type and riboflavin-producing *Bacillus subtilis*. Appl. Environ. Microbiol. 62, 3687–3696.

Sauer, U., Hatzimanikatis, V., Bailey, J.E., Hochuli, M., Szyperski, T., Wuthrich, K., 1997. Metabolic fluxes in riboflavin-producing *Bacillus subtilis*. Nat. Biotechnol. 15, 448–452.

Sauer, U., Lasko, D.R., Fiaux, J., Hochuli, M., Glaser, R., Szyperski, T., Wuthrich, K., Bailey, J.E., 1999. Metabolic flux ratio analysis of genetic and environmental modulations of *E. coli* central carbon metabolism. J. Bacteriol. 181, 6679–6688.

Sauer, U., Canonaco, F., Heri, S., Perrenoud, A., Fischer, E., 2004. The soluble and membrane-bound transhydrogenases UdhA and PntAB have divergent functions in NADPH metabolism of *E. coli*. J. Biol. Chem. 279, 6613–6619.

Schwender, J., Ohlrogge, J.B., Shachar-Hill, Y., 2003. A flux model of glycolysis and the oxidative pentose phosphate pathway in developing *Brassica napus* embryos. J. Biol. Chem. 278, 29442–29453.

Schwender, J., Goffman, F., Ohlrogge, J.B., Shachar-Hill, Y., 2004. Rubisco without the Calvin cycle improves the carbon efficiency of developing green seeds. Nature 432, 779–782.

Stephanopoulos, G., Aristidou, A.A., Nielsen, J., 1998. Metabolic Engineering: Principles and Methodologies. Academic Press, London.

Stouthamer, A.H., 1979. The search for correlation between theoretical and experimental growth yields. In: Quayle, J.R. (Ed.), International

Review of Biochemistry. Microbial Biochemistry, vol. 21. University Park Press, Baltimore.

Szyperski, T., 1995. Biosynthetically directed fractional ^{13}C-labeling of proteinogenic amino acids. An efficient analytical tool to investigate intermediary metabolism. Eur. J. Biochem. 232, 433–448.

Ullmann, R., Gross, R., Simon, J., Unden, G., Kroger, A., 2000. Transport of C_4-dicarboxylates in *Wolinella succinogenes*. J. Bacteriol. 182, 5757–5764.

van der Werf, M.J., Guettler, M.V., Jain, M.K., Zeikus, J.G., 1997. Environmental and physiological factors affecting the succinate product ratio during carbohydrate fermentation by *Actinobacillus sp*. 130Z. Arch. Microbiol. 167, 332–342.

van Winden, W., Verheijen, P., Heijnen, S., 2001. Possible pitfalls of flux calculations based on ^{13}C-labeling. Metab. Eng. 3, 151–162.

Venning, J.D., Jackson, J.B., 1999. A shift in the equilibrium constant at the catalytic site of proton-translocating transhydrogenase: significance for a 'binding-change' mechanism. Biochem. J. 341, 329–337.

Wahl, S.A., Dauner, M., Wiechert, W., 2004. New tools for mass isotopomer data evaluation in ^{13}C flux analysis: mass isotope correction, data consistency checking, and precursor relationships. Biotechnol. Bioeng. 85, 259–268.

Wendisch, V.F., de Graaf, A.A., Sahm, H., Eikmanns, B.J., 2000. Quantitative determination of metabolic fluxes during coutilization of two carbon sources: comparative analyses with *Corynebacterium glutamicum* during growth on acetate and/or glucose. J. Bacteriol. 182, 3088–3096.

Wiechert, W., 2001. ^{13}C Metabolic flux analysis. Metab. Eng. 3, 195–206.

Wiechert, W., de Graaf, A.A., 1997. Bidirectional reaction steps in metabolic networks: I. Modeling and simulation of carbon isotope labeling experiments. Biotechnol. Bioeng. 55, 101–117.

Wiechert, W., Siefke, C., de Graaf, A.A., Marx, A., 1997. Bidirectional reaction steps in metabolic networks: II. Flux estimation and statistical analysis. Biotechnol. Bioeng. 55, 118–135.

Wiechert, W., Mollney, M., Petersen, S., de Graaf, A.A., 2001. A universal framework for ^{13}C metabolic flux analysis. Metab. Eng. 3, 265–283.

Wilke, D., 1995. What should and what can biotechnology contribute to chemical bulk production? FEMS Microbiol. Rev. 16, 89–100.

Wilke, D., 1999. Chemicals from biotechnology: molecular plant genetics will challenge the chemical and fermentation industry. Appl. Microbiol. Biotechnol. 52, 135–145.

Wittmann, C., Heinzle, E., 2001. Application of MALDI-TOF MS to lysine-producing *Corynebacterium glutamicum*: a novel approach for metabolic flux analysis. Eur. J. Biochem. 268, 2441–2455.

Woehlke, G., Dimroth, P., 1994. Anaerobic growth of *Salmonella typhimurium* on L(+)- and D(−)-tartrate involves an oxaloacetate decarboxylase Na^+ pump. Arch. Microbiol. 162, 233–237.

Zamboni, N., Mouncey, N., Hohmann, H.P., Sauer, U., 2003. Reducing maintenance metabolism by metabolic engineering of respiration improves riboflavin production by *Bacillus subtilis*. Metab. Eng. 5, 49–55.

Zeikus, J.G., Jain, M.K., Elankovan, P., 1999. Biotechnology of succinic acid production and markets for derived industrial products. Appl. Environ. Microbiol. 51, 545–552.